to calculate the micelle hydrodynamic radius R_h^m. In view of eq 4, we have plotted $1/D_m$ vs. C_s in Figure 6. It can be seen that the plot is nearly linear and yields $D_m^0 = 7.4 \times 10^{-7}$ cm^2 s^{-1} and in turn $R_h^m = 30$ Å. This value agrees quite well with that which can be calculated for TTEAB micelles from their known aggregation number.[7]

The k_f coefficient obtained from the plot of Figure 6 cannot be given much significance, as it includes both the effect of intermicellar interactions and probe partitioning and will therefore not be discussed here.

Conclusions

The preliminary results reported in this paper show that dc polarography can be used to investigate the self-diffusion of ionic micelles tagged with an electroactive surfactant. The method is sensitive to the probe partition between micelles and the bulk, micelle size, and intermicellar interactions. The later effect results in a decrease of the measured diffusion coefficient upon increasing surfactant concentration, as observed in other studies of micelle self-diffusion. Future studies should focus on probes that are completely solubilized into the micelles, such as substituted polycyclic aromatic hydrocarbons. The complications arising from probe partitioning which greatly complicate the interpretation of the data would then be completely eliminated. Then, as the results presented in this paper suggest, valuable information on micelle size and intermicellar interactions will become available by means of polarography. It is noteworthy that this method is less expensive and/or generally less time consuming than other techniques presently used to measure micelle self-diffusion (pulsed field gradient Fourier transform NMR,[11c] capillary tubing with micelles tagged with radioactive labels,[11b] forced Rayleigh scattering,[11d] or fluorescence recovery after photobleaching[11e]) and represents an additional complementary and readily available technique.

Acknowledgment. We express their thanks to Dr. N. S. Dixit for his assistance in performing the measurements and to Dr. J. Candau for helpful discussions. The support of the U.S. Army Research Office is gratefully acknowledged.

Letters

Cluster Model and Charge Transfer in a Strong Metal–Support Interaction (SMSI) State

B. Viswanathan,*† Katsumi Tanaka,*‡ and Isamu Toyoshima‡

Department of Chemistry, Indian Institute of Technology, Madras 600 036, India, and The Research Institute for Catalysis, Hokkaido University, Sapporo 060, Japan

Received December 7, 1984. In Final Form: July 15, 1985

The model system Rh/SiO_x/n- or p-Si(111) was studied. Charge transfer from the support to the metal was ascertained in the Rh/SiO_x/n-Si(111) system by evaluating the Rh $M_5N_{4,5}N_{4,5}$ Auger peak shift and the XPS binding energy shift of Rh $3d_{5/2}$. Results are discussed together with consideration of a cluster model for the SMSI.

Introduction

When a group VIII (groups 8–10)[17] metal is dispersed atomically or in clusters on a support oxide matrix, namely, a model system for practical supported catalysts, the valence state of these dispersed species should be different from that of zero valency due to electronic interaction with species of the support. In a practical system, this type of interaction is usually induced by high-temperature pretreatment. However, this procedure is not suitable for model systems, because it will simultaneously induce other secondary effects like encapsulation, alloy formation, retention of species used for pretreatment, contamination, and segregation of impurities. The studies so far reported on the strong metal support interaction (SMSI) state[1] have this built-in multiplicity and hence could not be unequivocal regarding the electronic interaction and consequent charge transfer. In a previous paper,[2] we have modeled the SMSI state on the basis of a system consisting of $M/SiO_x/Si$ where M represents the transition metal; in this case it was nickel. The fabrication of this model system was achieved in such a way that the apparent metal support interaction effects were completely eliminated so that the effects observed could be ascribed only to the real metal–support interaction parameters involving electronic or geometric factors.[3] In this paper the results of similar measurements on the Rh/SiO_x/n- or p-Si model system are presented together with a consideration of cluster model for the SMSI state.

Experimental Section

The results reported in this paper were obtained with a VG ESCA 3 photoelectron spectrometer with analyzer chamber pressures typically in the order of (6–8) $\times 10^{-11}$ torr. All the XP

† Indian Institute of Technology.
‡ Hokkaido University.

(1) (a) Belton, D. N., Sun, Y. M.; White, J. M. *J. Phys. Chem.* **1984**, *88*, 1690. (b) Wang, J.; Lercher, J. A.; Haller, G. L. *J. Catal.* **1984**, *88*, 18. (c) Chung, Y. W., Xiong, G.; Kao, C. C. *J. Catal.* **1984**, *85*, 237.
(2) Viswanathan, B.; Tanaka, K.; Toyoshima, I. *Chem. Phys. Lett.* **1985**, *113*, 294.
(3) Bond, G. C.; Burch, R. "Specialist Periodical Reports, Catalysis"; The Royal Society of Chemistry: London, 1982; Vol. 6.

0743-7463/86/2402-0113$01.50/0

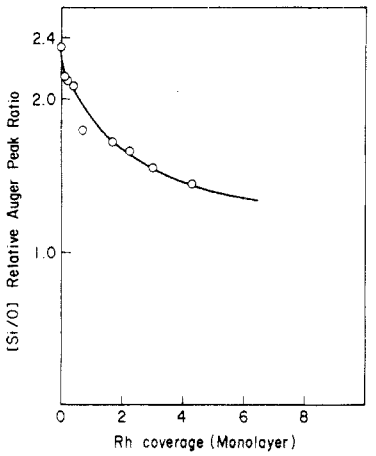

Figure 1. Variation of Si/O normalized Auger peak ratio as a function of rhodium coverage. The thickness of oxide layer was 4–5 Å.

spectra were recorded by using a Mg anode ($h\nu$ = 1253.6 eV), and the Auger lines were measured simultaneously with the same X-ray source. The binding energies observed were referenced to the 2p line of zero-valuent Si at 99.3 eV. Silicon(111) single crystals of n- or p-type obtained by doping with either P or B to the extent of 1×10^{16} atoms/cm^3 were used. Details of cleaning, formation, and characterization of the substrate, namely, SiO_x/n- or p-Si, are given in ref 2. The deposition of the metal on this substrate (typical rate 0.2–0.4 monolayer min^{-1}) was achieved by resistive heating of a tungsten filament. The cleanliness of the surface (with respect to carbon) was maintained at all stages of deposition with considerable care and effort. The calibration of surface coverage was done by the ideal layer-by-layer growth model and hence the absolute magnitudes are indicative values only by using a value 10 Å[4] for the electron inelastic mean free path for the Auger peak of rhodium at 302 eV (λ_{302}).

Results

The only apparent metal–support interaction effect that could have been present in this model system is encapsulation or oxide migration, where we assume the equivalent of the rhodium morphology on a n- or p-type silicon substrate. When the metal atoms condense on the substrate, the heat of concensation (~5.1 eV for Rh on Rh) is released and this could have been the driving force for encapsulation, oxide migration, or vacancy creation. The composition of the surface region was monitored from the Auger peak-to-peak amplitude (in the first derivative mode) of the oxygen (λ_{510}), rhodium (λ_{302}), and silicon (λ_{92}) peaks. In order to minimize the effects due to fluctuations in electron multiplier gain, the peak amplitudes were normalized to the sum of the three peaks (this was found to be approximately constant). The relative amplitudes of Si and oxygen peaks were thus computed. The inelastic mean free path for oxygen at 508 eV is enough to observe all of the oxygen in the silicon oxide layer formed (5 Å). Considering that the inelastic mean free path for Si at 92 eV is 39 A,[5] deposition of rhodium on the SiO_x/Si system should give rise to a decrease of the Si/O ratio. If encapsulation or oxide migration was to occur, then the Si/O ratio should have a flat region in the early stage of Rh deposition. The result of Figure 1 shows that no flat region was observed and hence it is unlikely that encapsulation was present in our model system. Encapsulation and oxide migration have been demonstrated in the case of the Rh/TiO_2 system by the variation of the Auger peak amplitude[6] which showed a maximum after initial increase or by the variation of Ti^+/Rh^+ ratio (as determined by static SIMS)[7] which showed initial decrease and constancy before increasing as a function of sputtering time. In view of these reports on Rh, the absence of encapsulation had to be established on our model system before identifying the real metal–support interaction effect.

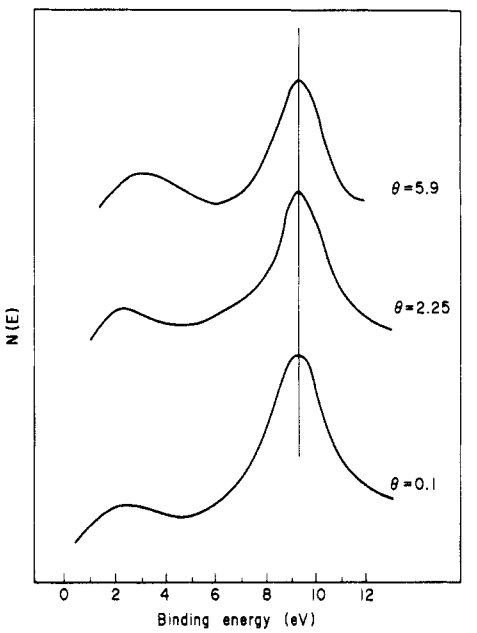

Figure 2. Valence band spectra of SiO_x/n-Si(111) substrate (4–5 Å thickness of oxide layer) as a function of rhodium coverage.

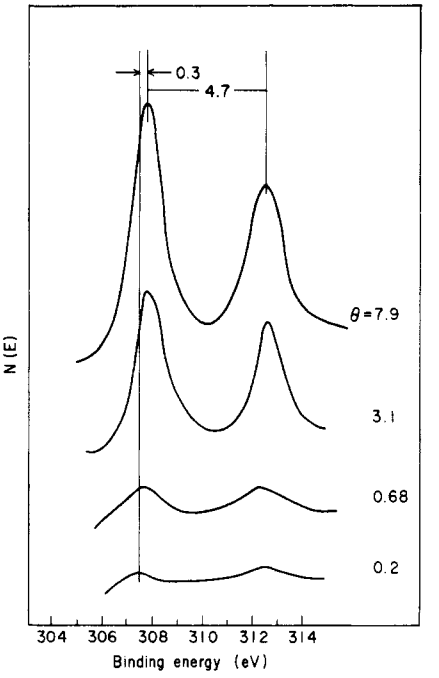

Figure 3. Rhodium $3d_{5/2}$ and $3d_{3/2}$ peaks for deposition on SiO_x/n-Si(111) substrate as a function of coverage. The thickness of oxide layer was 4–5 Å.

Figure 2 shows the valence band spectrum of the substrate used as a function of Rh coverage. In view of the multiphasic nature of our substrate, the absolute binding energy value alone is considered instead of referencing to the Fermi level. It can be seen that the valence level peak

(4) Seah, M. P.; Deneh, W. A. *SIA, Surf. Interface Anal.* **1979**, *1*, 2.
(5) Klasson, M.; Berndtsson, A.; Hedman, J.; Nilsson, R.; Nyholm, R.; Nordling, C. *J. Electron Spectrosc. Relat. Phenom.* **1974**, *3*, 427.
(6) Sadeghi, H. R.; Henrich, V. E. *J. Catal.* **1984**, *87*, 279.
(7) Belton, D. N., Sun. Y. M.; White, J. M. *J. Am. Chem. Soc.* **1984**, *106*, 3059.

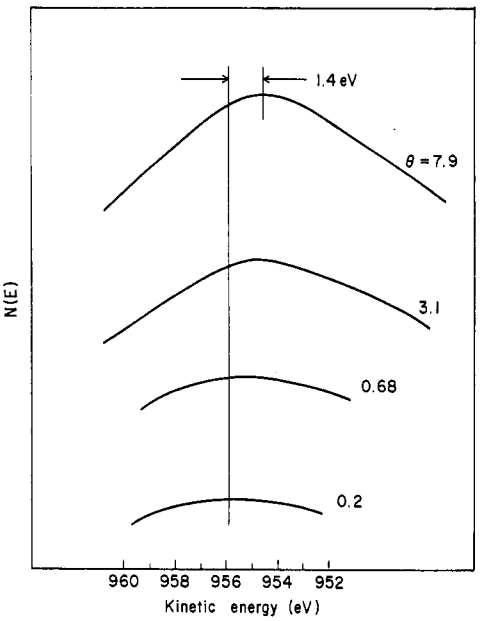

Figure 4. Rhodium $M_4N_{4,5}N_{4,5}$ peak on SiO_x/n-Si(111) substrate as a function of rhodium coverage. The thickness of oxide layer was 4–5 Å.

Table I. Rhodium $3d_{5/2}$ Binding Energy and $M_5N_{4,5}N_{4,5}$ Auger Peak Shifts as a Result of Rhodium Deposition on Oxide Substrate Formed on Si(111) Single Crystal, together with the Result for Ni[a]

	ΔBE/eV	ΔKE/eV	ΔE/eV	ΔR/eV
Rh/substrate				
thin oxide (~5 Å) on n-Si(111)	0.3 ± 0.1	−1.4	−0.25	−0.55
thin oxide (~5 Å) on p-Si(111)	0.1[b]	−0.5		
Ni/substrate				
thin oxide (~5 Å) on n-Si(111)	1.0	−4.0	−0.5	−1.5
thin oxide (~5 Å) on p-Si(111)	0.1[b]	−1.0		

[a] The alues of initial chemical shift ΔE and relaxation shift ΔR were calculated by the relations reported:[8] $\Delta BE = \Delta E - \Delta R + \Delta E_{bending}$; $\Delta KE = -\Delta E + 3\Delta R - \Delta E_{bending}$. Charge transfer from the support to the metal was defined by a negative value of ΔE. [b] Since these values are within our experimental accuracy, they are not considered. ΔBE and ΔKE values were taken between θ(coverage of metal) = 10 and the lowest θ value that could be measured that is ~0.2. The results of nickel were taken from ref 2.

is attenuated with increasing rhodium coverage but the position of the peak is not altered and emission in the band gap region is clearly seen with increasing rhodium coverage. The observation that the band bending is almost negligible is consistent with results reported in the literature.[1,8]

The Rh $3d_{5/2}$ peak shifts to lower binding energy values (Figure 3) while the $M_5N_{4,5}N_{4,5}$ Auger peak shifts to higher kinetic energy values (Figure 4) with increasing Rh coverage. These observations are similar to those reported in the literature.[2,8] In order to extract the initial state chemical shift parameter, ΔE, deduced by the method reported by Chung et al. (shown in Table I), we used the relation that the Auger parameter $\Delta\alpha = 2\Delta R$, where ΔR is extent of relaxation. This is a simple relation taking into account only the first-order terms for the relaxation effect. In the experimental situations that one has in the SMSI state this relationship does not take into account parameters like change in the valence charge as a result of core

(8) (a) Bahl, M. K.; Tsai, S. C.; Chung, Y. W. *Phys. Rev. B* **1980**, *21*, 1344. (b) Kao, C. C., Tsai, S. C.; Chung, Y. W. *J. Catal.* **1982**, *73*, 136.

Table II. Summary of XPS Studies of Rhodium Loading on Various Supports

support[c]	binding energy shift or value of Rh $3d_{5/2}$, eV	reason	ref
ZnO	307.1	Rh–Zn bond	9
TiO_2	−0.7,[a] −0.2[b]	charge transfer	10
TiO_2 (2)	−0.6[a]	charge transfer	11
V_2O_5 (1)	−0.3[a]	charge transfer	11
Ta_2O_3 (1)	0.0[a]		11
Nb_2O_3 (1)	−0.3[a]	charge transfer	11
HfO_2 (1)	0.0[a]		11
TiO_2	0.0	encapsulation and spalling at higher temp	12
Al_2O_3	0.0	no charge transfer	12

[a] Initial values. [b] After cycling. [c] Values in parentheses refer to % dispersion.

ionization, and so the magnitude of chemical shift observed cannot be used to evaluate the net charge transfer from the support to the metal. The magnitude of these parameters is summarized in Table I together with the values obtained for Ni or SiO_x/Si system.[2]

Discussion

The XPS studies of rhodium on the other supports reported in the literature so far are summarized in Table II. Wehner et al.[9] observed that there is a buildup of intensity at the higher kinetic energy side of the Zn $L_3M_{4,5}M_{4,5}$ peak indicating the reduction of Zn^{2+} to Zn^0, and, since this reduction is not feasible under the conditions employed by them in the case of pure ZnO, they conclude that rhodium should be stabilizing Zn^0 probably in the form of alloy. However, in their experiments, hydrogen spillover could have been the cause for the observed small (~0.2 monolayer) reduction of ZnO. Both Haller et al.[10] as well as Sexton et al.[11] have recorded a minimum chemical shift of −0.2 ± 0.5 eV after cycling of oxidation and reduction pretreatments, though the initial chemical shift value was as high as −0.6 eV in the case of TiO_2. This expected value of the true chemical shift is in agreement with observations of the Rh/SiO_x/Si model system, since reduction pretreatment is eliminated in this system by the design. Sexton et al.[11] propose that the reduction in chemical shift values as a result of cycling could be due to particle size variations and morphology changes. It should be remarked that Prins et al.[12] have not observed any shift in the binding energy of Rh $3d_{3/2}$ peak as a result of high-temperature reduction. Sexton et al. also have made an estimate of 0.5 eV for the relaxation shift, which is in agreement with the value observed for our model system. It is therefore probable that, in our model system, charge transfer from the support to the metal does occur though the extent can be far less than 0.5 eV per rhodium atom as predicted by Sexton et al.[11]

In order to account for our observations we propose the following cluster model for the SMSI state. It is known that high-temperature reduction of supported systems results in partially reduced states of the support and consequently there may be changes in the interfacial energy that favor wetting of the support by the metal species[13] which spread and form certain morphological pat-

(9) Wehner, P. S.; Apai, G. A.; Mercer, P. N. *J. Catal.* **1983**, *84*, 244.
(10) Chen, S. H.; Shelimov, B. N.; Resasco, D. E.; Lee, E. H.; Haller, G. L. *J. Catal.* **1982**, *77*, 301.
(11) Sexton, B. A.; Hughes, A. E.; Foger, K. *J. Catal.* **1982**, *77*, 85.
(12) Huizinga, T.; Vant Blick, H. F. J.; Vis, J. C.; Prins, R. *Surf. Sci.* **1983**, *135*, 580.

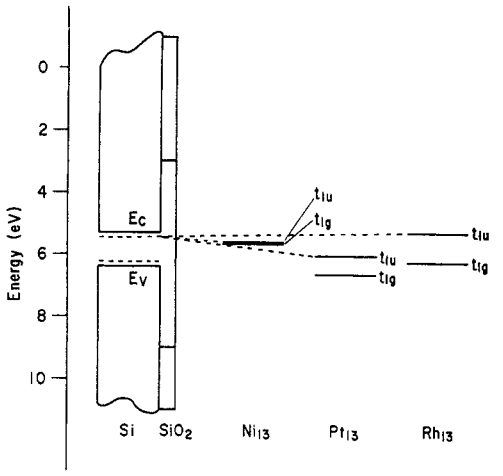

Figure 5. Energy level diagram for the model system $M/SiO_x/Si$. For the 13-atom metal clusters only the highest occupied (t_{1g}) and lowest unoccupied (t_{1u}) are shown by a single horizontal line for clarity. The energy values are as per $X\alpha$ calculations. For details of calculational procedure see ref 16. E_c and E_v represent the energetic position of conduction band and valence band edges.

terns. Recent EXAFS studies on supported systems[14,15] favor metal cluster formation as a result of high-temperature hydrogen reduction. Though these studies postulate a 13-atom cluster as the most probable species, the size and number for distribution of clusters are dependent on a number of parameters including the nature of the support, the conditions used for reduction and its extent (which alters the value of the interfacial energy), the nature of the metal used, and the method of loading. As a typical case, a 13-atom cubooctahedral cluster formation is considered though the treatment may equally be valid for other cluster sizes. The energy level diagram for the model system, namely, $M/SiO_x/Si$, is given in Figure 5.

In the case of a 13-atom cluster for Ni, Rh, and Pt, the states that are of relevance for our consideration are the HOMO and LUMO levels with t_{1g} and t_{1u} symmetry. In the case of nickel clusters, these two sets of levels are degenerate and are partially occupied, thus accounting for the paramagnetism. In the case of Rh and Pt clusters, the t_{1g} levels with pure "d" character are fully occupied, while the t_{1u} levels with "dsp" character are completely empty. As the oxide has a forbidden gap in this energy range, the relative positions of these levels with respect to the donor states of n-type silicon favor charge transfer by tunneling. The extent of charge transfer as deduced from the magnitude of the difference in t_{1u} energy levels and donor states should be in the order Pt > Ni > Rh, provided that a collective electron model is chosen. The reverse charge transfer is not possible in the case of Rh and Pt as the HOMO levels, namely, t_{1g} levels, are below the possible acceptor states in p-type silicon. Though in the case of nickel one can expect the reverse charge transfer due to the relative positions of the acceptor states and the lowest unoccupied states, this is not observed because of the low mobility of the charge carriers in the metal cluster and the localized nature of the cluster states and possibly due to differences in symmetry of the wavefunctions of the acceptor levels and the metal cluster. This cluster model can account for the following observations on the SMSI state:

(1) The occupancy of t_{1u} states accounts for the suppression in chemisorption capacity for CO or H_2 in the SMSI state as these states are no longer available for charge-transfer interaction with valence levels (5σ or 1π) of the molecules.

(2) The extent of charge transfer will be dependent on the density of donor states and the charge transfer will be distributed among the various metal atoms in the cluster, thus accounting for partial (<1e/metal atom) charge on the metal atoms.[8]

Acknowledgment. We acknowledge with thanks the fellowship to one of us (B.V.) from the Japan Society for the Promotion of Sciences (JSPS). We also thank Dr. Yatsurughi, Komatsu Electronics Japan, for kindly supplying n- and p-type silicon single crystals. This work was partially supported by Grant in Aid for Scientific Research (No. 5670062) from the Ministry of Education of Japan (I.T.)

Registry No. SiO_x, 11126-22-0; Rh, 7440-16-6; Si, 7440-21-3.

(13) Baker, R. T. "Studies in Surface Science in Catalysis"; Elsevier: Amsterdam, 1982; Vol. 11, p 37. "Metal Support and Metal Additive Effects in Catalysis"; Imelik, B., et al., Eds.; Elsevier: Amsterdam, 1982.
(14) Logarde, P.; Murata, T.; Vlaic, G.; Freund, E.; Dexpert, H.; Bornonville, J. P. *J. Catal.* **1983**, *84*, 333.
(15) Sinfelt, J. H., Via, G. H.; Lytle, F. W. *J. Chem. Phys.* **1982**, *76*, 2779.
(16) Messmer, R. P.; Knudson, S. K.; Diamond, J. B.; Yang, C. Y. *Phys. Rev. B* **1976**, *13*, 1396.
(17) In this paper the periodic group notation is modified in accord with recent actions by IUPAC and ACS nomenclature committees. A and B notation is eliminated because of wide confusion. Groups IA and IIA become groups 1 and 2. The d-transition elements comprise groups 3 through 12, and the p-block elements comprise groups 13 through 18. (Note that the former Roman number designation is preserved in the last digit of the new numbering: e.g., III → 3 and 13.)